Annals of Biomedical Engineering (© 2022)
https://doi.org/10.1007/s10439-022-03026-8

S.I. : Modeling for Advancing Regulatory Science

In Silico Fit Evaluation of Additively Manufactured Face Coverings

Ian A. Carr,[1] Gavin D'Souza,[1] Ming Xu,[2] Shailesh Ozarkar,[2] Daniel Porter,[1] Marc Horner,[2] and Prasanna Hariharan[1]

[1]Division of Applied Mechanics, Office of Science and Engineering Laboratories, Center for Devices and Radiological Health, United States Food and Drug Administration, 10903 New Hampshire Avenue, Silver Spring, MD 20993, USA; and [2]Ansys Inc., 1007 Church Street, Suite 250, Evanston, IL 60201, USA

(*Received 21 April 2022; accepted 14 July 2022*)

Associate Editor Stefan M. Duma oversaw the review of this article.

Abstract—In response to the respiratory protection device shortage during the COVID-19 pandemic, the additive manufacturing (AM) community designed and disseminated numerous AM face masks. Questions regarding the effectiveness of AM masks arose because these masks were often designed with limited (if any) functional performance evaluation. In this study, we present a fit evaluation methodology in which AM face masks are virtually donned on a standard digital headform using finite element-based numerical simulations. We then extract contour plots to visualize the contact patches and gaps and quantify the leakage surface area for each mask frame. We also use the methodology to evaluate the effects of adding a foam gasket and variable face mask sizing, and finally propose a series of best practices. Herein, the methodology is focused only on characterizing the fit of AM mask frames and does not considering filter material or overall performance. We found that AM face masks may provide a sufficiently good fit if the sizing is appropriate and if a sealing gasket material is present to fill the gaps between the mask and face. Without these precautions, the rigid nature of AM materials combined with the wide variation in facial morphology likely results in large gaps and insufficient adaptability to varying user conditions which may render the AM face masks ineffective.

Keywords—COVID-19, Face mask, Additive manufacturing.

INTRODUCTION

The COVID-19 pandemic put unprecedented strains on the production of personal protective equipment (PPE). Perhaps the most salient category of PPE to both the public and healthcare workers is respiratory protective equipment, e.g. face masks and respirators. As part of the response to PPE shortages, many additive manufacturing (AM) face mask designs have been developed, disseminated, and studied. Herein, we present a numerical simulation-based methodology to assess and improve the design of AM face mask frames along with a series of general design recommendations.

AM techniques have found numerous uses during the supply shortages caused by COVID-19. Face-shield frames, valve adaptors for respirators, devices to augment the fit of surgical masks, along with the facemask frames evaluated in this research work have been designed and made available by the AM community. A review by Longhitano et al. provides an overview of the COVID-19 activity by the AM community.[16] Similar reviews by Advincula et al. and Tino et al. provide broad overviews of the uses, challenges, and recommendations associated with the use of AM techniques to adapt to the difficulties of the COVID-19 pandemic.[2, 24]

Swennen et al. published one of the earliest works detailing an AM face mask frame in response to COVID-19 related supply shortages.[22] This proof of concept used the replaceable filter from an FFP2/3 respirator. To achieve a better fit and less leakage, Swennen et al. used 3D facial scanning and a Boolean calculation to produce a frame profile specific to the wearer. A similar technique was used to achieve a user-specific fit in Shaheen et al. [21] Subjective user reports from these studies show that user-specific designs increase comfort and improve fit. Both studies note however that the primary obstacle to distributing user-specific AM face masks frames is the need to acquire

Address correspondence to Ian A. Carr, Division of Applied Mechanics, Office of Science and Engineering Laboratories, Center for Devices and Radiological Health, United States Food and Drug Administration, 10903 New Hampshire Avenue, Silver Spring, MD 20993, USA. Electronic mail: ian.carr@fda.hhs.gov

Published online: 28 July 2022

the 3D facial data for each user. The time, and in some cases equipment, required for this step slows the pace at which masks of this style can be produced and distributed. Other studies have found that even with CT-based, user-specific designs, AM mask frames were unable to pass quantitative respirator fit testing.[3] For distribution at any considerable scale, non-user specific designs offer a compelling alternative if the performance issues associated with inferior fit and comfort can be addressed. The fit evaluation methodology presented in this study can be used to evaluate the fit characteristics of both general purpose and user-specific face mask frame designs.

Simulation-based methodologies using finite-element analysis (FEA) have been previously developed to study the comfort and fit of traditional N95 respirator. Lei et al. studied the contact pressure between a standard headform and an N95 respirator.[15] Xu et al. studied the dead space volume between a headform and an N95 respirator after donning the respirator.[26]

The limited literature investigating the effectiveness of AM face masks reports mixed results. This is to be expected for a variety of reasons. For example, AM manufacturing techniques enable extremely wide variation in design and implementation and thus wide variation in performance. The effectiveness is further complicated by characteristics which make face mask design inherently inconsistent: anatomical diversity and poor mask conformability, e.g., gaps between the mask and face, which result in dramatically reduced performance.[6, 19] These two factors are compounded when the user is moving or speaking while wearing a rigid AM mask frame. In spite of these known issues, Chichester et al. showed that AM face masks can attain a fit factor nearly equivalent to an N95 respirator if proper care is taken by a trained user using good mask frame design, careful post-processing, and a high-quality filter material.[5] But Duda et al. showed extremely low effectiveness in real-world use of a wider selection of mask designs.[9] These two studies clearly illustrate the need to consider not only the design of AM masks but also the realities and limitations of real-world use.

In this study, we focus on the AM face mask frame only. We do not consider the filter material insert or the overall performance of the completed AM face-mask. Therefore, when designing an AM face mask frame, the computational methodology presented in this study could be used in tandem with the selection of a suitable filter material. If possible, these frames should be paired with an application-specific commercial filter material, e.g., melt blown polyethylene fabric, rather than woven fabric or other ad hoc filter materials. If purpose-made filter materials are not available, then there is a wealth of literature on the filtration efficiency and breathability of common materials.[12, 14, 27] As with all face masks, the effectiveness is dependent on all aspects of the design—fit, filtration, and breathability—working in concert to trap airborne particles.

The design methodology presented herein is not an alternative to quantitative fit testing, e.g., OSHA protocol 29CFR1910.134.[18] Rather, this methodology should be used in tandem with quantitative fit testing to iteratively improve AM face mask design. Several studies have used quantitative fit testing to evaluate mask fit and some have included discussion of the possible locations and severity of the leakage gaps [19, 25]. Using the techniques presented in this study, AM mask frame designers can precisely locate and quantify the area of the gaps, alter their design, then perform particle concentration-based quantitative fit testing on the revised design.

The next section summarizes the FEA methodology that can be used to assess and modify the fit of AM face mask frames before 3D printing. While the evaluation and visualization methodology is our primary contribution, we also demonstrate the utility of the methodology by applying it to several mask frame designs and characteristics. The Results section summarizes how the methodology reveals the effects of frame design, variable sizing, and fit modifications on the ability of a given face mask design to conform to the wearers face. The methodology is also used to examine the impact of headform size on fit performance. In the Discussion section, these results are used to assess implications of variations in mask design and head shape/size and to propose a series of general good practice recommendations.

MATERIALS AND METHODS

This section outlines the FEA-based methodology to assess the fit of AM face mask frames. The methodology consists of virtually donning a frame onto a rigid digital headform using a two-part FEA simulation. A rigid headform, as opposed to a more complex, compliant headform, is used to maintain the simplicity and accessibility of the evaluation method. Once donned the resultant areas of mask frame-to-headform contact and gaps are visualized using contour plots and the total area of the gaps is also quantified. A validation study using additively manufactured headforms and masks is also summarized.

Four representative face mask frame designs were obtained from the National Institutes of Health (NIH) 3D Print Exchange, see Fig. 1.[25] The mask frame designs were selected early in the COVID-19 pandemic

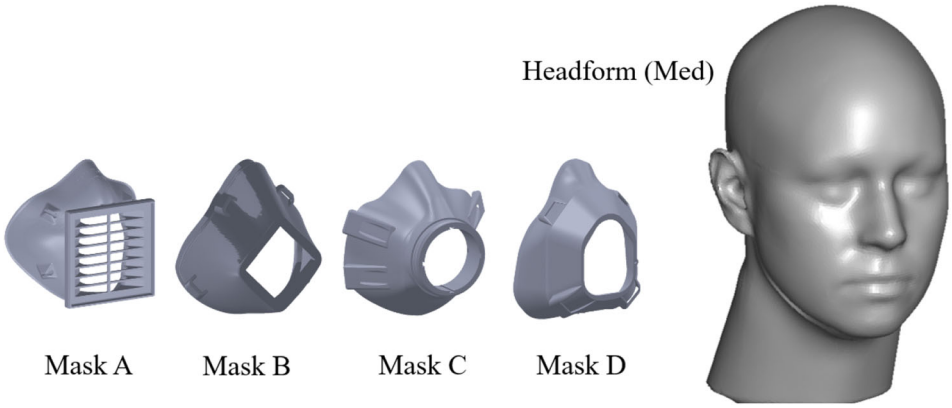

FIGURE 1. The four AM mask designs evaluated in this study along with an example NIOSH standard, medium-sized headform. See the following references for further details on the mask frames: Mask A,[20] Mask B,[11] Mask C,[1] Mask D [17].

based on popularity, which was judged by the number of downloads on popular online 3D printing repositories. When these designs were originally accessed (Spring 2020), two of the mask frame designs were offered in multiple sizes (Mask A in small, medium, and large and Mask B in small and large) while the other two mask frame designs (Mask C and D) were only offered in a single size resulting in 7 total mask frames included in the study. The mask frames were fitted to National Institute for Occupational Safety and Health (NIOSH) digital headform models, sizes small, medium, and large.[28]

All simulations were performed using Ansys LS-Dyna R11.1.0 software (Ansys, Inc. Canonsburg, PA) with pre- and post-processing performed using Ansys LS-PrePost V4.7.8 software (Ansys, Inc. Canonsburg, PA). The mask frame geometries were meshed in Ansys SpaceClaim 2021 R1. Each mask frame was composed of roughly 100,000 elements with an averaged element size slightly less than 1 mm. Our mesh refinement study was comprised of seven meshes of progressively smaller element size. It showed that the total contour area (in which the contact gap was between 0 and 5 mm) changed less than 1% when the mesh was refined past roughly 1 mm mesh elements indicating mesh convergence. The computer used to run the simulations is equipped with an 8-core 3.6 GHz Intel Core i9 processor with 32 GB of RAM. The headform and strap computational meshes were created in Ansys LS-PrePost.[10]

Following Xu et al., the simulations were composed of two parts: Part 1. A strap tensioning simulation in which the straps are pulled around the headform to meet with the frame attachment points tensioning the straps (see Fig. 2).[26] Part 2. A mask donning simulation in which the straps are attached to the frame and the preexisting tension in the straps pulls the mask to the headform (see Fig. 3). This two-part simulation protocol ensures the mask frame-headform interface is faithfully recreated and allows the mask frame to settle into a natural resting position before the subsequent analysis is performed. Allowing the mask frame to slide against the face also lessens the influence of the initial position of the mask frame.

In LS-Dyna, the contact conditions between parts were managed using a variety of protocols depending on the requirement. In Part 1, the contacts between the straps and headforms were handled using the Automatic Surface-to-Surface process. While in Part 2, the contacts between the mask frame and headform were handled with Automatic Surface-to-Surface MORTAR to allow control of the range of detectable gaps in the final contact-gap contour. The straps were connected to the mask in Part 2 by connecting nodes on the attachment points on the mask to the nodes at the end of the strap. When appropriate, the foam gasket was added between Parts 1 and 2 using a Tied Surface-to-Surface contact. The Tied Surface-to-Surface contact had a slight offset to ensure the foam gasket was adhered to the mask but would be allowed to slide against the headform as necessary.[10]

The material properties used in the simulations were based on the materials used in the validation experiments. The mask frame and straps were modeled using an isotropic hypoelastic material model (LS-Dyna MAT_001). The foam gasket was modeled using a highly compressible low density foam model (LS-Dyna MAT_057) using the experimental loading curve data from Croop and Lobo.[7] Material property data for the mask frame material and strap material is provided in Table 1. All face mask frame models were assigned the material properties of polyethylene terephthalate glycol (PETG), the material used in the validation experiments. Using the same material for all masks has the benefit of facilitating comparisons of the results from the different frames tested. Each mask frame is composed of approximately 200,000 tetrahedral elements. The headform is modeled as a rigid body. The

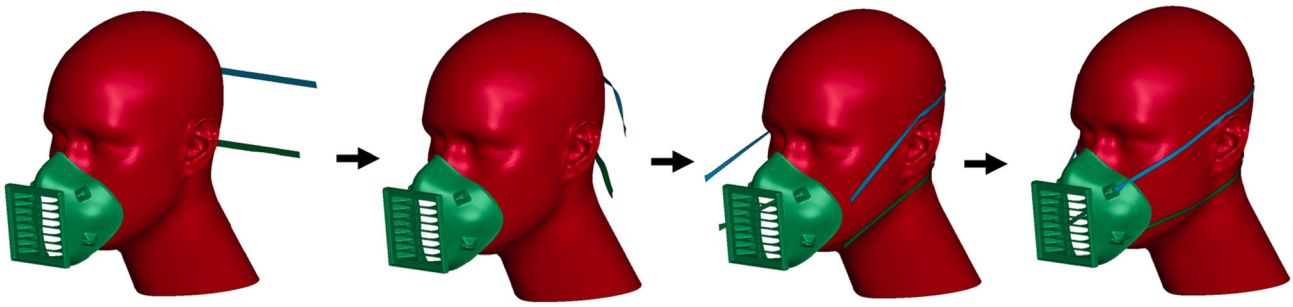

FIGURE 2. Part 1 of the FEA simulation: strap tensioning simulation.

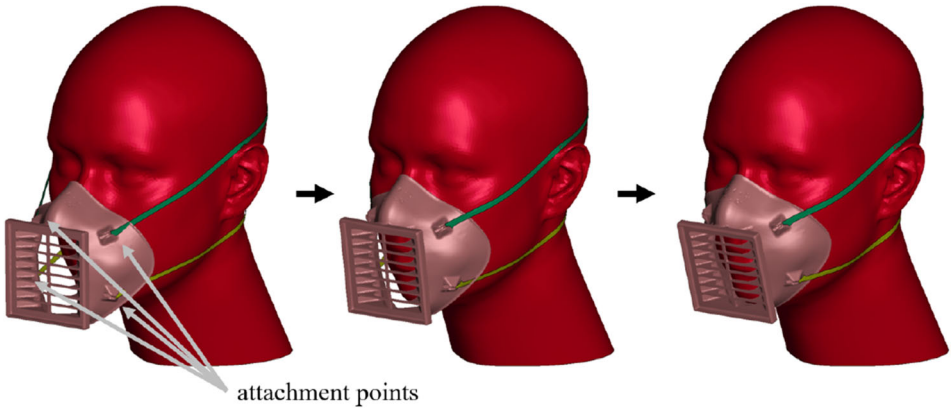

FIGURE 3. Part 2 of the FEA simulation. From left to right: strap attachment, mask pulled towards headform by strap tension, mask sliding on headform and settling into place.

TABLE 1. Simulated material properties of the AM material and strap material.

	PETG (frame)	Latex (straps)[23]
Density (kg/m^3)	1270	60
Young's Modulus (MPa)	1500	3
Poisson's Ratio	0.4*	0.49

*Properties of the filament before printing.

straps which pull the frame to the headform are modeled using shell elements. When the face mask frame reaches its final position the simulation is stopped and the Contact Gap fringe visualization is used to produce the contour maps of the distance between the face mask frame and digital headform.

Once the mask reaches its final position on the headform, the resultant geometry is used to calculate the total surface area of each gap between the mask and headform using Materialise 3-matic software (Materialise, Inc., Lueven, Belgium). A four-step procedure is followed to determine the leakage gap surface area (see Fig. 4): (1) Locate the contact patches and gaps on the headform. (2) Determine the position of the line of minimum distance between two adjacent contact patches. (3) Construct a plane along the line of minimum distance which is perpendicular to the surface of the headform. (4) Calculate the area on the perpendicular plane between the lines of intersection with the headform and face mask frame geometries. This process is carried out for each gap for a given face mask frame and headform combination. These values are subsequently summed to calculate the leakage gap surface area.[8, 13]

The following measures are used to assess the fit for various frame designs (1) contact gap profile between the face mask and the headform and (2) surface area of the leakage gap created due to imperfect fit.

Validation

We use a series of paint-based visualizations to validate the outputs of the numerical model. Headforms and mask frames were generated using in-house 3D printing. While the AM mask frames deflect when donned, the AM headform model has thick walls making it effectively rigid for this application—matching the simulated rigid headform in the numerical model. An even layer of water-soluble paint was applied to the edges of the mask frame or foam gasket. We then fit the mask to the headform, transferring the paint from mask to headform where the mask is in contact with the headform. The resulting

contact patch visualization was compared to the wetted area visualization in the simulation (i.e., a contour of the region in which the mask frame and headform were in contact at any time in the simulation). While qualitative in nature, this visualization-based validation provides evidence that the simulations are faithfully recreating the contact patch between the mask frame and headforms. We assume the validity of the simulated contact patches indicates the validity of the gap profiles.

Note: Both the numerical simulations and experimental validation are based on rigid headforms and consequentially both do not recreate real facial tissue with its variable deformability. The aim of the experimental validation is to validate the in-silico design methodology, not to validate the numerical simulations to real world conditions.

Figure 5 shows two instances of the validation procedure performed using Mask A. In Fig. 5a, the contact locations are highlighted by blue paint. Figure 5b is the corresponding wetted area visualization from the simulation in which the contact locations are highlighted in red. Note the similarity in the primary contact patches: the center of the nose bridge, the upper cheek bones, lower cheeks and three distinct areas on the chin. Figure 5c shows the complete contact patch when the mask frame is fitted with a highly compressible foam gasket. Similarly, Fig. 5d shows the simulated wetted area visualization for the same mask frame with foam. These visualizations demonstrate that the simulations are faithfully recreating the contact patch locations which implies the simulated gap profiles are similarly accurate.

RESULTS

In this section, we use a series of contact-gap contours to visualize and evaluate the size and location of the contact patches and gaps between the mask frames and the rigid headform. Along with the simulation methodology presented above, the visualization methodology presented below is designed to allow AM mask designers to identify design flaws and improve

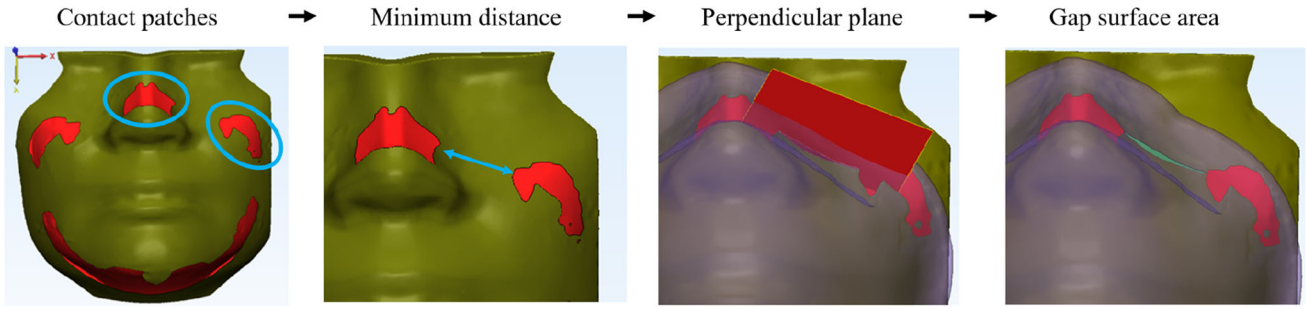

FIGURE 4. Four-step procedure to calculate the leakage gap surface area. This process was carried out for all gaps in a given headform—face mask frame combination.

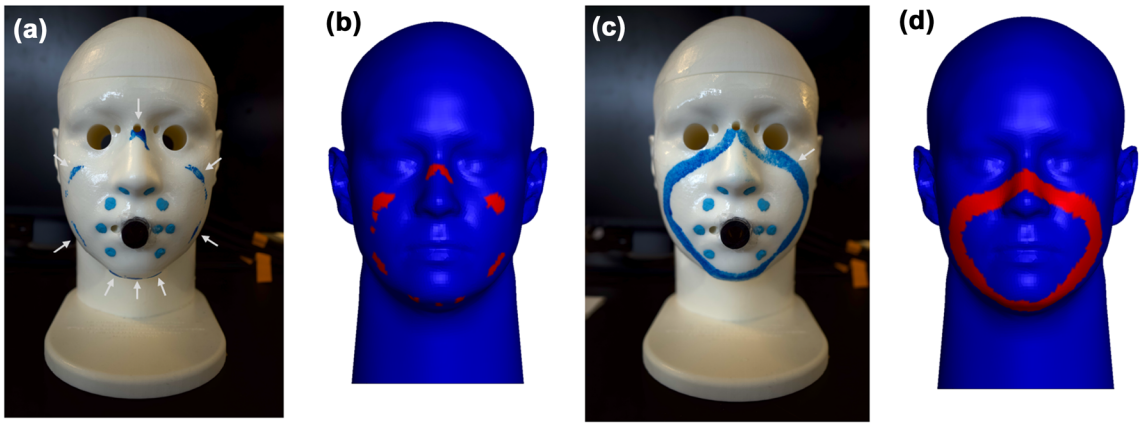

FIGURE 5. Paint-based experimental validation. (a) Mask A paint visualization, contact patches highlighted with arrows. (b) Mask A simulated wetted area visualization. (c) Mask A with foam gasket paint validation, contact patches highlighted with arrows. (d) Mask A with foam gasket simulated wetted area visualization. *Note*: the small, light blue dots surrounding black mouth port are not contact patches.

the fit of their masks. To demonstrate the utility of this technique, we will evaluate the impact of a sample of frame designs, the effects of adding a foam gasket after printing, and the effects of multi-sized mask designs on mask fit performance.

Facemask Frame Design

In this section, we compare the fit of four facemask frame designs on a size medium NIOSH digital headform. A colorbar is used to indicate the distance between the headform and the mask frame (*cf* Fig. 6): black indicates full contact (0.0 mm gap), green indicates a moderate gap height between 1.5 and 3.5 mm, red indicates a large gap, and light grey (a gap in the contour map itself) indicates a gap of larger than 5.0 mm. Therefore, a perfect fit would appear as an unbroken black contour extending around the perimeter of the mask frame-headform interface. In Fig. 6, and all subsequent contact-gap figures, the headforms are tilted vertically upwards by 20° to more easily observe the contact-gap contours.

The contact-gap contour plots in Fig. 6 elucidate the locations of the contact patches and gaps between the mask and face, and also conveys the overall quality of fit of the selected mask frame designs on a medium headform. As is clear from Fig. 6, no mask frame design evaluated here achieved a perfect fit since gaps can be identified for each mask.

Mask A has the best fit on the standardized headform with the only significant gaps on either side of the nose bridge. Mask B achieves slightly better fit around the nose bridge, but has substantial gaps on the lower cheeks. Mask C has several large gaps primarily near the cheek bones and on top of the nose. Mask D, the worst fit for this headform, has gaps larger than 5 mm on the lower cheeks and on the top of the nose.

The overall impression of the quality of the fit portrayed in Fig. 6 is borne out in the leakage gap surface area quantification, which is summarized in Table 2. The computational model predicts that Mask A has the lowest leakage gap surface area with the largest gaps around 1.5 mm on either side of the nose. If the model headform was composed of real, deformable tissue then Mask A would likely fit well. Masks B and C have similar leakage gap surface areas, which are both predicted to be 3–4× that of Mask A, with the majority of the gap regions around 3.0 mm. Mask D has the largest leakage gap surface area—roughly 20× the gap area of Mask A.

Effects of a Foam Gasket

In this section, we use the computational model to evaluate the role which minimal augmentations to the rigid AM masks can play in modifying the fit of the masks on the rigid headforms. Specifically, we simulate the addition of a 6.35 mm thick, 12.7 mm wide (1/4 inch by 1/2 inch), highly deformable foam gasket along the interior edge of the mask. Typically, these foam gaskets take the form of an adhesive-backed foam strip applied by hand.

Given the rigidity of many popular print materials along with the wide variation in face shapes, it is intuitive that the introduction of structural compliance via a foam gasket could have a large beneficial effect on mask contact performance. The contact-gap profiles shown in Fig. 7 confirm this intuition, which shows how the addition of the foam gasket eliminates the gaps completely for all masks tested. As shown in

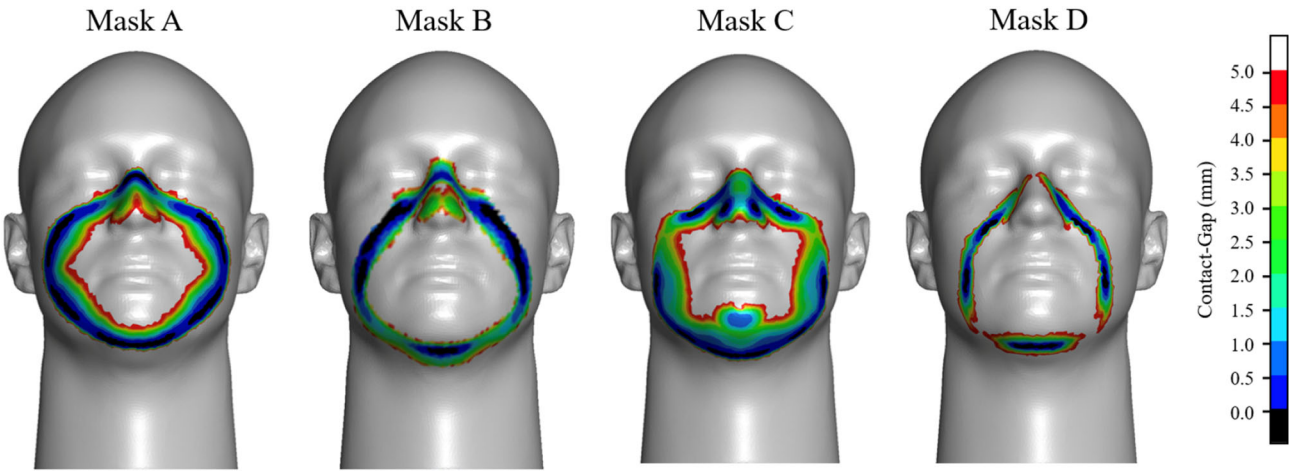

FIGURE 6. Contact-gap contour maps of the face mask frame designs shown in Fig. 1. The areas in black indicate contact between the frame and headform, the areas of green, yellow, and red indicate gap heights between 2.0 and 5.0 mm, and light grey (the base color of the headform) in the contour indicate a gap larger than 5.0 mm between the mask frame and headform.

TABLE 2. Leakage gap surface area of the mask frames shown in Fig. 6.

	Mask A	Mask B	Mask C	Mask D
Leakage gap surface area (mm^2)	89.9	395.3	271.9	1669.8

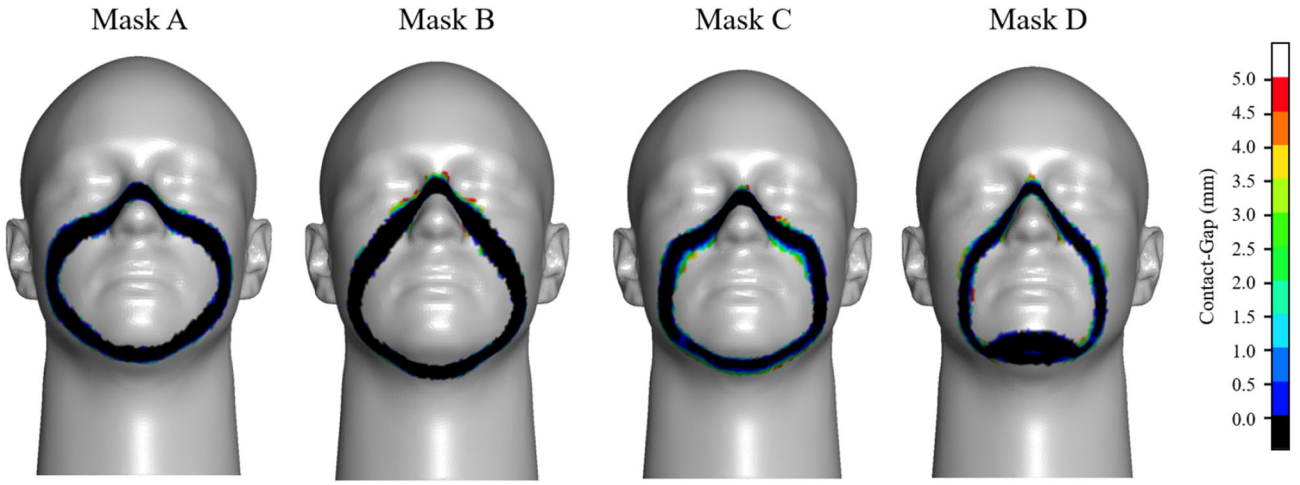

FIGURE 7. Contact-gap profiles for four primary mask designs with foam gasket fitted to mask. This treatment reduced the leakage gap surface area to 0.0 mm^2 for each mask.

Table 2, the resultant leakage gap surface area is predicted to be zero for all four mask frame designs.

Effects of Variable Sizing

In this section, we evaluate the role of variable sizing in AM mask designs on contact performance. Two of the mask designs evaluated are available in multiple sizes (Masks A and B), while the other two are available in a single size (Mask C and D). While intuition suggests that variable sizing will improve fit on headforms of various sizes, contact-gap contours can provide clear, quantitative evidence.

In Fig. 8 we compare the fit of Mask C, which has one size, to Mask A, which comes in 3 sizes, on NIOSH standard headforms sized small, medium, and large. In the case of Mask A, each headform was fitted with the corresponding size mask, i.e. small mask on small headform, medium mask on medium headform, and large mask on large headform.

The contact-gap contours in Fig. 8 demonstrate the benefits of designing an AM mask frame in multiple sizes. The locations of contact patches and gaps for Mask C are inconsistent across headform sizes and relatively large in all cases, as is shown in Table 4. The quality of fit of Mask C is predicted to be the best on the medium headform with 271.9 mm^2 of total leakage gap surface area—a value more than double any case in Mask A fitted to the corresponding headforms. The fit of Mask C on the small and large headforms is significantly degraded, exhibiting large gaps in several locations. This contrasts with the Mask A studies, which exhibit a significantly lower total leakage area for all headform sizes.

DISCUSSION

This study uses computational modeling to simulate the interaction between four AM face mask frames and digital headforms from NIOSH. An experimental investigation of the contact points provided validation data that justifies the model predictions. The contact-gap contours derived from the numerical simulations provided a more detailed view of the headform-mask frame interface than our experiments could provide. Our work shows that AM face masks with a rigid frame fitted to rigid headforms do not typically provide a sufficiently good fit without further alteration or augmentation of the mask frame. This is in agreement with other literature on the limitations of fit and performance of AM face mask frames [3, 4]. The contact-gap profiles in Fig. 6 reveal the location of the gaps and the degree of design modification required to improve fit. This test is particularly unforgiving in that neither the headform nor the mask frame have considerable compliance or deformability which would

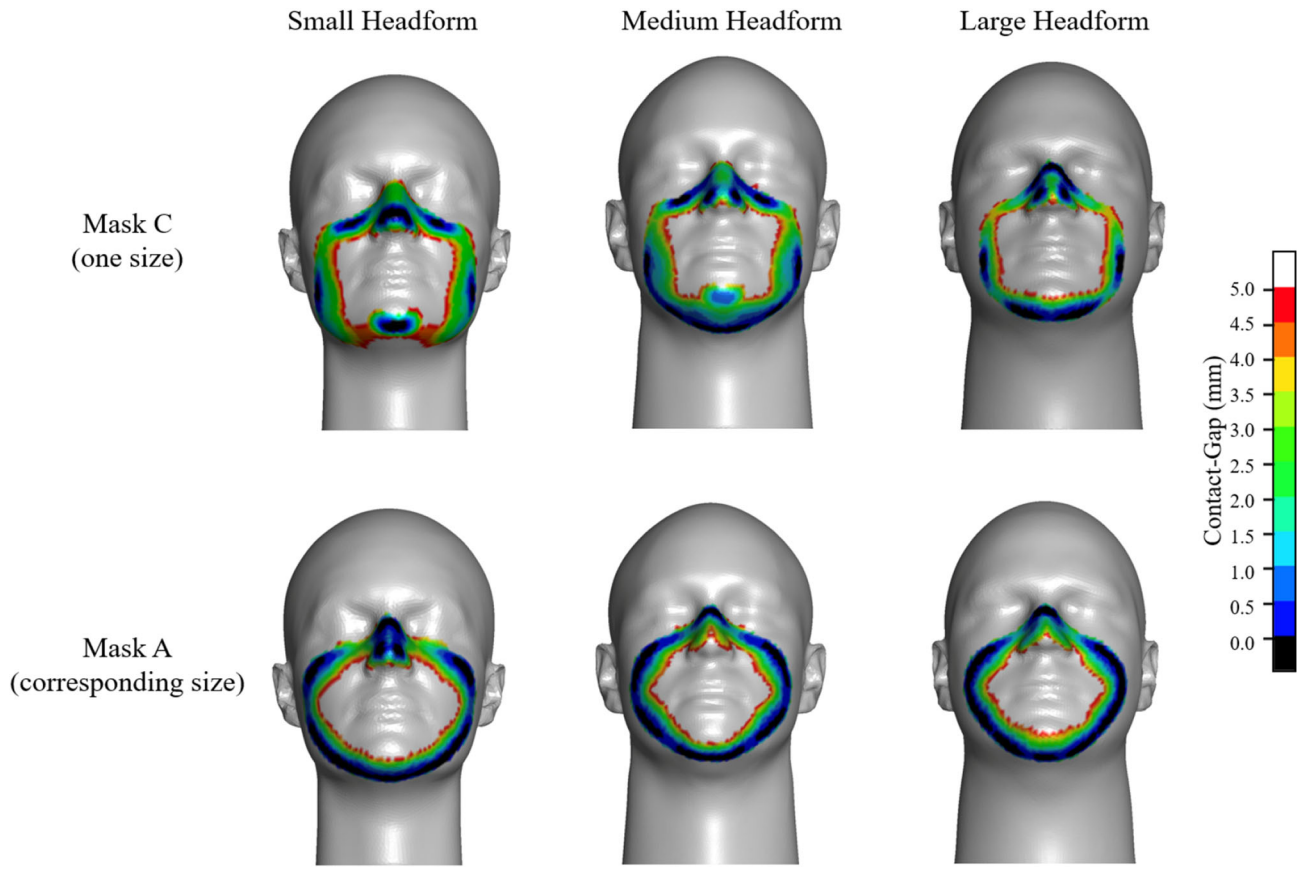

FIGURE 8. Comparison of mask frame fit of a single-sized mask frame against a mask frame with variable sizing. The top row shows contact-gap contours on small, medium, and large headforms from Mask C (one-size). The bottom row shows contact-gap contours from Mask A using the size corresponding to the size of the headform.

improve the seal between the mask and the face. Real facial tissue would deform filling some of the gaps, but likely not the largest. Moreover, the diverse morphology of real faces would produce other contact-gap patterns resulting in widely varying quality of fit.

For a sense of scale, the leakage gap surface area of Mask D in Table 1 is roughly equivalent to the area of 3.5 US Quarters. Similarly, the leakage gap surface area for Mask B is roughly the area of a single US Nickel. Put differently, this is roughly similar to a perfectly fitted mask having a US Nickel sized hole cut into it. Gaps of this scale likely result in little flow through any highly effective filter material, significantly reducing the masks effectiveness.

Note the variation in the total width of each contour, i.e., the distance from the inner diameter to outer diameter. This can be thought of as the potential contact patch since real tissue is deformable and would occupy some of the smaller gaps. A mask frame with a larger overall contact patch would exert less pressure on the face increasing the comfort of the wearer. Using this assumption, Masks A and C would likely be more comfortable than Masks B and D.

Our analysis of the four sample AM face mask frames indicates that further augmentations will be needed to make them safe to distribute. While the results of this study only pertain to AM face mask frames, the benefits of fit augmentations demonstrated in Fig. 7 agree with other studies on fit augmentations of more traditional face coverings.[25] Without augmentations, the rigid nature of AM materials tends to result in large gaps between the mask frame and headform and inconsistent fit across facial morphologies. More specifically, Fig. 7 and Table 3 show how the addition of a foam gasket significantly improves fit. Along with the improved fit on an immobile, rigid simulated headform, the addition of a foam gasket likely has other real-world benefits. The foam gasket allows AM masks to accommodate a larger diversity of facial morphologies. The compliance of the foam gasket would also improve the fit across a variety of wearer conditions: looking up, down, left or right; speaking; coughing and sneezing, etc. While only shown to be beneficial to general purpose face mask frames in this study, the performance of user-specific face mask frames (e.g., those designed with 3D scan-

ning) would likely also be improved by the adaptability to user conditions afforded by a foam gasket. It is important to select a gasket material which is both highly deformable and non-porous, e.g., a foam gasket with large, open cells may produce good fit but allow leakage through the material itself making it a poor gasket material. Lastly, the addition of a foam gasket will likely improve comfort for the wearer, especially if the foam is fitted such that it covers the outer edge of the frame.

While the results displayed in Fig. 7 and Table 2 make a compelling case for the addition of a foam gasket there are important caveats. The foam gasket can only fill gaps smaller than its uncompressed height which was 6.35 mm in this case. While we did not observe gaps this large in our sample of mask frame designs, certain mask frame-face combinations with gaps larger than the thickness of the foam gasket could easily occur. Therefore, the thickness and placement of the foam gaskets should be considered alongside the design and wearer-specific criteria. Additionally, our simulations only indicate contact between the mask frame and headform, but not necessarily an airtight seal. There is still the possibility of leakage between the mask frame and headform if the foam is only lightly contacting the headform. The increased pressure inside the mask due to exhalation may also cause leakage if the foam gasket is only lightly contacting the headform. This is especially true if the filter material paired with the frame requires a high pressure drop for a typical rate of respiration, or if the wearer is at an elevated rate of respiration.

The results in Fig. 8 and Table 4 demonstrate the benefits of designing multiple sizes of AM face mask frames. The quality of the fit using Mask A in the corresponding size is superior in several ways. Across headform sizes, the location of the contact patches and gaps is consistent with a leakage gap surface area below 100 mm^2 in all cases. This suggests that when fitted with a foam gasket, or other fit augmentations, the improvement in fit would apply to a wider variety of face sizes. With the addition of a foam gasket, the primary gaps in both cases around the nose bridge would be eliminated.

The results shown in Fig. 8 also elucidate the drawbacks of supplying only one size of AM face mask. The fit of Mask C varies widely across headform sizes. Namely, while Mask C makes relatively even contact with the medium headform, Mask C's contact patches on the small and large headforms are small and separated by large regions not in contact with the headform. This results in large leakage gap surface areas in both cases. Not only would this make for a poor fit and likely excessive leakage, but the small contact patches likely translate to uncomfortable pressure points on the wearers face. Specifically, Mask C contacts the small headform in a localized region on the chin and on the tip of the nose. Similarly, the contact patches on the large headform are primarily on the nose bridge and chin.

This analysis shows that providing an AM mask frame in multiple sizes can greatly improve fit across a wider diversity of face shapes. This intuitive result is backed up by quantitative measures. In any circumstance where AM face masks are distributed at scale, providers should use a design that is either user-specific or available in a wide variety of sizes. Moreover, the real-world diversity of facial morphology extends far past the small, medium, and large models analyzed in this study. This should also be reflected in the number of versions available to users if AM masks are distributed at any large scale. As with the application of a

TABLE 3. Leakage gap surface area of the mask frames with the addition of a foam gasket shown in Fig. 7.

	Mask A	Mask B	Mask C	Mask D
Leakage gap surface area (mm^2)	0.0	0.0	0.0	0.0

TABLE 4. Leakage gap surface area of the masks shown in Fig. 8.

	Small headform	Medium headform	Large headform
Mask C Leakage gap surface area (mm^2)	822.9	271.9	340.5
Mask A Leakage gap surface area (mm^2)	97.2	89.9	31.9

foam gasket, the sizing of a mask should be iterative and based on feedback from the users.

To summarize, the rigid nature of most AM materials does not lend itself to a consistently good fit on the wide diversity of facial morphologies and wearer conditions. Using the computational assessment methodology presented in this study may provide an evaluation method that supports design improvements to AM face masks. This framework could be used as a design, testing, and selection tool to evaluate the fit quality offered by new and existing AM face masks before going through additive manufacturing and validation bench testing. Along with improved design, the addition of a foam gasket or other gasket material along with a wide array of available sizes, are both strongly recommended if producing or using rigid AM face mask frames. Without these precautions, rigid AM face masks can have very poor fit with large gaps between the mask and face, likely translating to poor overall performance. As such, if these precautions cannot be met, rigid AM face masks may not be appropriate and carry the risk of providing a false sense of protection against viral aerosols and droplets.

Limitations of Study

The objective of this study is to present a relatively simple and accessible method to evaluate and improve AM mask frame designs before production. To achieve this relative simplicity, the headform is modeled as a rigid material. A rigid material model was used in place of a more realistic, deformable headform model because of the complexity involved in modeling organic tissue, especially facial tissue with its wide variation in deformability and depth to bone. One consequence of modeling a rigid headform is to make achieving a good fit more difficult as there is no deformable facial tissue to occupy small gaps. In this sense, this is a conservative evaluation methodology in which the fit may be better in practice than it appears using this method.

Another limitation of this study is the use of a standard headform model which does not account for anatomical variation. The NIOSH standard digital headforms serve as an averaged, generic facial geometry which clearly does not represent all potential wearers.[28] As such, we do not claim that the quantitative values of leakage gap surface area or the exact contact-gap contour maps will be representative of a particular wearer. Rather, we present the evaluation methodology along with three general recommendations (variable sizing, a gasket material, and iterative design based on user feedback) and show a sample of cases to demonstrate the legitimacy of these recommendations.

Lastly, the design methodology presented herein only assesses the quality of the face-mask frame interface, not the overall performance of an AM face mask, and is not a replacement for quantitative fit testing. Accordingly, this methodology should be considered alongside the multitude of studies which focus only on the filtration efficiency of materials.[12, 14, 27] When designing a high-quality AM face mask, a mask designer may use the design methodology presented to refine the mask frame design, select a well-established, highly efficient filter material, and perform rigorous quantitative fit testing on the resultant AM mask design.

ACKNOWLEDGMENTS

Disclaimer: The findings presented here do not represent any determination or policy of the Food and Drug Administration. Any mention of commercial products in this paper is not to be construed as an endorsement by the Department of Health and Human Services.

FUNDING

A portion of the funding supporting this project was provided by the Oak Ridge Institute for Science and Education.

CONFLICT OF INTEREST

IC, GD, MX, SO, DP, MH, and PH declare no conflicts of interest. No benefits of any form have been or will be received from a commercial party related to the contents of this manuscript. MX, SO, and MH are salaried employees of Ansys Inc.

REFERENCES

[1]3DP. Coronavirus COVID reusable washable face respirator mask. Prusa Printers, 2020. [Online]. https://www.prusaprinters.org/prints/26047-coronavirus-covid-reusable-washable-face-respirato. Accessed Sept 2021.

[2]Advincula, R., J. R. C. Dizon, Q. Chen, I. Niu, J. Chung, L. Kilpatrick, and R. Newman. Additive manufacturing for COVID-19: devices, materials, prospects, and challenges. *MRS Commun.* 10:413–427, 2020.

[3]Ballard, D. H., U. Jammalamadaka, K. W. Meacham, M. J. Hoegger, B. A. Burke, J. A. Morris, A. R. Scott, Z. O'Conner, C. Gan, J. Hu, K. Tappa, R. Wahl, and P. J. Woodard. Quantitative fit tested N95 respirator-alternatives generated with CT imaging and 3D printing: a response to potential shortages during the COVID-19 pandemic. *Acad. Radiol.* 28(2):158–165, 2021.

[4]Bezek, L. B., J. Pan, C. Harb, C. E. Zawaski, B. Molla, J. R. Kubalak, L. C. Marr, and C. B. Williams. Additively manufactured respirators: quantifying particle transmission and identifying system-level challenges for improving filtration efficiency. *J. Manuf. Syst.* 60:762–773, 2021.
[5]Chichester, D. L., J. D. Hix, J. T. Johnson, L. A. Ocampo Giraldo, S. M. Watson, B. T. Mortensen, and C. Z. Angell. Evaluation of an additively manufactured respirator for personnel protection from particulates. Idaho Falls: Idaho National Laboratory, 2020.
[6]Chiera, S., A. Cristoforetti, L. Benedetti, G. Nollo, L. Borro, L. Mazzei, and F. Tessarolo. A simple method to quantify outward leakage of medical face masks and barrier face coverings: implication for the overall filtration efficiency. *Int. J. Environ. Res. Public Health*. 19:3548, 2022.
[7]Croop, B., and H. Lobo. Selecting material models for the simulation of foams in LS-Dyna. In: 7th European LS-Dyna conference, 2009.
[8]D'Souza, G., S. Guha, M. Myer, and P. Hariharan. Evaluation of aerosol leakage sites through respirators using image-based modeling. In: ASME front biomed devices, 2017.
[9]Duda, S., S. Hartig, K. Hagner, L. Meyer, P. Intriago Wessling, T. Meyer, and H. Wessling. Potential risks of a widespread use of 3D printing for the manufacturing of face masks during the severe acute respiratory syndrome coronavirus 2 pandemic. *J 3D Print Med.* 2020. https://doi.org/10.2217/3dp-2020-0014.
[10]DYNAmore GmbH. LS-Dyna support, 2022. [Online]. https://www.dynasupport.com/manuals. Accessed Dec 2020.
[11]Fiedler, M. FlexFit face mask, 2020. [Online]. https://3dprint.nih.gov/discover/3dpx-014173. Accessed Sept 2021.
[12]Guha, S., A. Herman, I. A. Carr, D. Porter, R. Natu, S. Berman, and M. R. Myers. Comprehensive characterization of protective face coverings made from household fabrics. *PLoS ONE*. 13(16):13, 2021.
[13]Hariharan, P., N. Sharma, and S. Guha. A computational model for predicting charges in infection dynamics due to leakage through N95 respirators. *Sci. Rep.* 11:10690, 2021.
[14]Kwong, L. H., R. Wilson, S. Kumar, Y. S. Crider, Y. R. Sanchez, D. Rempel, and A. Pillarisetti. Review of the breathability and filtration efficiency of common household materials for face masks. *ACS Nano*. 15:5904–5924, 2021.
[15]Lei, Z., J. Yang, and Z. Zhuang. Headform and N95 filtering facepiece respirator interaction: contact pressure simulation and validation. *J. Occup. Environ. Hyg.* 9(1):46–58, 2012.
[16]Longhitano, G. A., G. B. Nunes, G. Candido, and J. V. L. da Silva. The role of 3D printing during COVID-19 pandemic: a review. *Progress Addit. Manuf.* 6:19–37, 2021.
[17]Maker Mask. "Maker Mask," Maker Mask, 2020. [Online]. https://www.makermask.com/. Accessed Sept 2021.
[18]Occupational Safety and Health Administration. Appendix A to section 1910.134—fit testing procedures (mandatory), 2004. [Online]. https://www.osha.gov/laws-regs/regulations/standardnumber/1910/1910.134AppA.
[19]O'Kelly, E., A. Arora, S. Pirog, J. Ward, and P. J. Clarkson. Comparing the fit of N95, KN95, surgical, and cloth face masks and assess the accuracy of fit checking. *PLoS ONE*. 2021. https://doi.org/10.1371/journal.pone.0245688.
[20]Richburg, C. Stopgap surgical face mask (SFM), 2020. [Online]. https://3dprint.nih.gov/discover/3dpx-01349. Accessed Sept 2021.
[21]Shaheen, E., R. Wilaert, I. Miclotte, R. Coropcuic, M. Bila, and C. Politis. A novel fully automatic design approach of a 3D printed face specific mask: proof of concept. *PLoS ONE*. 2020. https://doi.org/10.1371/journal.pone.0243388.
[22]Swennen, G. R. J., L. Pottel, and P. E. Haers. Custom-made 3D-printed face masks in case of pandemic crisis situations with a lack of commercially available FFP2/3 masks. *Int. J. Oral Maxillof. Surg.* 49:673–677, 2020.
[23]Texter, J., N. Tambe, R. Crombez, M. Antonietti, and C. Giordano. Stimuli responsive coatings of carbon nanotubes and nanoparticles using ionic liquid-based nanolatex. *Polym. Mater.: Sci. Eng.* 102:401–402, 2010.
[24]Tino, R., R. Moore, S. Antoline, R. Prashanth, N. Wake, C. N. Ionita, J. M. Morris, S. Decker, A. Sheikh, F. Rybicki, and L. L. Chepelev. COVID-19 and the role of 3D printing in medicine. *3D Print Med.* 2020. https://doi.org/10.1186/s41205-020-00064-7.
[25]U.S. Department of Health and Human Services - National Institute of Health. NIH 3D print exchange, 2021. [Online]. https://3dprint.nih.gov/. Accessed Dec 2020.
[26]Xu, M., Z. Lei, and J. Yang. Estimating the dead space volume between a headform and N95 filtering facepiece respirator using microsoft kinect. *J. Occup. Environ. Hyg.* 12(8):538–546, 2015.
[27]Zangmeister, C. D., J. G. Radney, E. P. Vicenzi, and J. L. Weaver. Filtration efficiencies of nanoscale aerosol by cloth mask materials used to slow the spead of SARS-CoV-2. *ACS Nano*. 14:9188–9200, 2020.
[28]Zhuang, Z., and B. Bradtmiller. Head-and-face anthropometric survey of U.S. respirator users. *J. Occup. Environ. Hyg.* 2(11):567–576, 2005.